Anal. Methods Environ. Chem. J. 8 (4) (2025) 38-46

AMECJ

Research Article, Issue 4
Analytical Methods in Environmental Chemistry Journal
Journal home page: www.amecj.com/ir

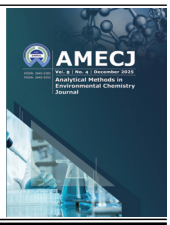

Electrochemical Analysis: Fabrication and evaluation of Ag/Ni catalysts based on TiO_2 nanotubes for sodium borohydride oxidation

Fatemeh Zeraatpisheh[a,*], Maryam Nourozizadeh[a], Ismaeil Mohammadi[b], Saeid Khodadoust[a]
[a]*Department of Chemistry, Behbahan Khatam Alanbia University of Technology, Behbahan, Iran.*
[b]*Laboratory, Persian Gulf Bidboland Gas Treating Company, Behbahan, Iran*

ARTICLE INFO:
Received 3 Aug 2025
Revised form 28 Oct 2025
Accepted 17 Nov 2025
Available online 28 Dec 2025

Keywords:
Anodizing,
Direct borohydride fuel cell,
Electrochemical analysis,
Fuel cell,
Nanoparticle.

ABSTRACT
In this research, titanium dioxide nanotubes (TiO_2-NTs) were synthesized by anodization on a titanium (Ti) sheet. Then, nickel (Ni), silver (Ag), and Ag/Ni nanoparticles were deposited on TiO2-NTs via electrochemical deposition. X-ray diffraction (XRD) and scanning electron microscope (SEM) were used to characterize the synthesis of TiO_2-NTs and nanoparticles deposited on TiO_2-NTs. SEM images and XRD data indicated that the nanotubes were well synthesized, and the Ni, Ag, and Ag(Ni) particles were well dispersed on their surfaces. In the next step, the electrocatalytic activity of the synthesized catalysts (TiO_2-NTs, Ni/TiO_2-NTs, Ag/TiO_2-NTs and Ag (Ni)/TiO_2-NTs) in relation to $NaBH_4$ (at four concentrations 0.00, 0.01, 0.03 and 0.05 M of $NaBH_4$) oxidation were examined by various methods including: chronoamperometry (CA), chornopotantiometry (CP), cyclic voltametry (CV), linear sweep voltametry (LSV). These experiments showed that bimetallic electrocatalysts (Ag(Ni)/TiO_2-NTs) are more efficient than monometallic electrocatalysts. The results showed that bimetallic electrodes are more efficient in the electrooxidation of borohydrate.

1. Introduction

Mastery of energy is always the key to a better world. Energy can manifest in many forms, such as chemical, electrical, mechanical, radiant, nuclear, and thermal. For example, in an electric vehicle, a battery converts chemical energy into electrical energy, which is then converted into mechanical energy by an engine. The term energy was first used in a practical sense by Young (1829-1773), who provided the most accurate definition: energy is the ability to do work. It is usually stated that (work) means trying to do something, and the amount of work done is called (power). Therefore, devices consume energy, do work, and produce power [1-5]. Hydrogen (H_2) is an ideal, renewable, and clean energy source and a promising alternative to fossil fuels in the future. Currently, a large amount of consumed H_2 comes from natural gas reforming; however, this process does not reduce the dependence on fossil fuels and produces carbon dioxide (CO_2) [6, 7]. Likewise, the use of sodium borohydride ($NaBH_4$) as an alternative fuel for H_2 production has attracted the attention of many researchers since its discovery. A fuel cell is an electrochemical device that produces electricity as long as a fuel and an oxidizer are supplied. Today, several types of fuel cells are being developed, each with its own advantages and disadvantages. These fuel cells differ depending on working temperature, fuel, catalyst, and other parameters. Fuel cells directly convert chemical energy into electrical energy. One type of fuel cell is

*Corresponding Author: Fatemeh Zeraatpisheh
Email: fzeraatpisheh@gmail.com
https://doi.org/10.24200/amecj.v8.i04.1053

the direct borohydride fuel cell (DBFC), which has recently been considered as a significant option for transportation applications. DBFC is a promising technology for meeting the energy requirements of portable electronic applications [8, 9]. This fuel cell has special features that make it a promising power source for portable applications. These features include: High energy density (9.3 Wh/g from V1.64), low toxicity of reagents and their products, easy storage, 4) their stability in alkaline solution [1], and ease of transporting BH_4^- [3]. The operation of DBFC is usually based on the oxidation of BH4-, including 8 electrons in the anode (Equation 1) and the reduction of oxygen in the cathode (Equation 2) [10]. The general reaction is depicted in Equation 3.

$$BH_4^- + 8OH^- \rightarrow BO_2^- + 6H_2O + 8e^- \quad E^0 = -1.24\ V_{VS.SHE} \quad \text{(Eq.1)}$$

$$2O_2 + 4H_2O + 8e^- \rightarrow 8OH^- \quad E^0 = 0.4\ V_{VS.SHE} \quad \text{(Eq.2)}$$

$$BH_4^- + 2O_2 \rightarrow BO_2^- + 2H_2O \quad E^0 = 1.64\ V \quad \text{(Eq.3)}$$

Noble metals such as Pt and Au have been investigated as anodes for the oxidation of BH4- in DBFC. However, compared to Pt, which is a detrimental catalyst for the hydrolysis reaction of BH4-, Au shows a high Coulombic efficiency for the oxidation reaction of BH4- (BOR). However, the use of Au as an electrode is limited by its high cost. One way to reduce the Au content is to disperse Au nanoparticles on a substrate. Recently, Au alloys with transition metals such as Ni [11], Co [12], and Cu [13]
have been reported to reduce costs and improve catalytic performance for BOR. It has been found that binary metal catalysts usually have higher activity and stability than monometallic ones [6–8]. Furthermore, binary catalysts offer significant advantages, as they exhibit many interesting size-dependent electrical, chemical, and optical properties. Bimetallic catalysts, especially their nanoparticle form, are exciting, as they are usually composed of a primary metal that has high electrocatalytic activity and a secondary metal that can enhance the catalysts' efficiency towards BOR or inhibit BH4- BH4-hydrolysis [14-17]. The transition metal can also be doped with a noble metal to reduce the catalyst's cost. Moreover, transition metals can be doped with one another to achieve higher electrocatalytic activity through complex synergistic effects [18-24]. The main purpose of this study is to investigate the mono or bimetallic catalyst nanoparticles for BOR electrooxidation in DBFC. We synthesized TiO_2-NTs anodes with deposited Ni, Ag, and Ag(Ni) for BOR using an electrochemical deposition method. SEM and XRD were used to characterize the morphology and crystalline structure of the synthesized catalysts. The electrocatalytic activity of the synthesized catalysts was investigated using various electrochemical methods, including chronoamperometry (CA), chronopotentiometry (CP), cyclic voltammetry (CV), and linear sweep voltammetry (LSV).

In our study, we focused on the preparation of titanium oxide-doped nanoparticles with Ni, Ag, and Ag(Ni) to exploit their catalytic activity for hydrogen production. The TiO_2 nanotubes prepared by electrospinning are considered the best candidate for use as a host material due to their good mechanical and thermal properties [2, 6]. Furthermore, this study indicates that bi-metallic doping of TiO_2 nanotubes increased the TiO2 surface area, thereby leading to a higher rate of hydrogen generation.

2. Experimental

2.1. Materials

$NaBH_4$ (98%; CAS No.: 16940-66-2), $AgNO_3$ (CAS No.: 7761-88-8), $Ni(NO_3)_2$ (CAS No: 13478-00-7), $NaNO_3$ (CAS No.: 7631-99-4), HF (CAS No.: 7664-39-3), NH_4F (CAS No.: 12125-01-8), HNO_3 (CAS No.: 7697-37-2), NaOH (CAS No.: 1310-73-2), KOH (CAS No.: 1310-58-3), ethanol (CAS No.: 64-17-5), acetone (CAS No.: 67-64-1) and ethylene glycol (CAS No.: 107-21-1) were purchased from Merck Company (Germany). Deionized water was used to prepare the electrolyte solution.

2.2. Making the catalyst

The catalysts were prepared through a three-step process that included Ti anodization (TiO_2-NTs), Ni

and Ag electrochemical deposition on TiO_2-NTs, and Ag electrochemical deposition on the Ni/TiO_2-NTs. First, after sanding and degreasing the Ti sheet, it was placed in a solution containing 98 mL of ethylene glycol, 2 mL of deionized water, and 0.3 g of NH_4F, and anodizing was performed with a constant voltage of V = 50 for 4 hours at 25 ºC. After anodizing, the Ti sheet on which nanotubes (TiO_2-NTs) were synthesized was washed and dried, then placed in an ultrasonic bath containing C_2H_5OH and distilled water for 2 minutes; the Ti was washed, dried, and placed in a zip-lock bag. For the Ni and Ag address layer, the TiO_2-NTs electrode was placed in a solution of 0.5 M $Ni(NO_3)_2$ and 0.1 M $NaNO_3$, and a Pt counter electrode was used. Electrochemical analysis was performed for 180 seconds by the CP test at -1 mA. To make the Ag(Ni)/TiO_2-NTs catalyst, the Ni coating electrode was done with the same method as above, then the Ni/TiO2-NTs electrode was placed in the electrolyte containing 0.005 M $AgNO_3$ and 0.1 M $NaNO_3$, and the electrochemical analysis was performed with the CHP test for 120 seconds at -1 mA. The morphology and composition of the catalysts were determined by scanning electron microscopy (SEM) and X-ray diffraction (XRD). XRD analyses were performed in 0 – 80 ◦2θ range using XRD XPert Pro MPD, with X-ray source: Cu Kα radiation (Kα =1.54187 Å).

2.3. Electrochemical measurements

DBFC experiments were performed using Ni/TiO_2-NTs, Ag/TiO_2-NTs, and Ag(Ni)/TiO_2-NTs catalysts with a surface area of 2.0 cm^2, with these catalysts used as working electrodes and Pt as the counter electrode. The oxidation of $NaBH_4$ has been carried out in four electrolytes with different concentrations (including 1 M KOH (without $NaBH_4$), 0.01 M, 0.03 M, and 0.05 M $NaBH_4$) to determine the optimal concentration for the highest oxidation efficiency of $NaBH_4$. All measurements were performed using an electrochemical device with 4 tests: linear scan voltammetry (LSV), cyclic voltammetry (CV), chronopotentiometry (CP), and chronoamperometry (CA). For all experiments, the desired solution was poured into the cell as the electrolyte, the catalyst was connected to the system as the working electrode, Pt as the counter electrode, and Ag/AgCl electrode as the reference electrode. The electrochemical measurements were performed using the Sama 500 Electro Analyzer (Iran). The LSV test was performed at E1 = -1V, E2 = 0.5V, and a scan rate of 0.05V/s. The CV test was performed at currents I_1 = -1mA, I_2 = 0.5 mA, and I_3 = -1mA and scan rate = 0.05 V/s. The CP test was performed with E1 = -1V and E2 = 0.5V for 300 seconds. The CA test was performed at voltages E_1 = -1V and E_2 = 0.5V for 300 seconds.

3. Results and discussion

3.1. Physical characteristics

In this research, TiO_2-NTs, Ni/TiO_2-NTs, Ag/TiO_2-NTs, and Ag(Ni)/TiO_2-NTs catalysts were synthesized by the electrochemical method and investigated as anodes in $NaBH_4$ direct fuel cell (DBFC). First, TiO_2-NT arrays were prepared by anodizing a Ti sheet in a solution of ethylene glycol and water containing NH_4F. According to SEM images (Fig. 1A), the average diameter of TiO_2 nanotubes (TiO_2-NTs) is 100 nm with a thickness of 4.7 µm. According to the SEM images, the nanotubes are well-formed and uniformly distributed on the Ti surface. The Ni/TiO_2-NTs catalyst was made by layering Ni nanoparticles on TiO_2-NTs. According to the SEM images shown in Figure 1B, the average diameter of the Ni nanoparticles is 52 nm, with a thickness of 7.3 µm. The SEM images of the Ag/TiO_2-NTs electrode with an average diameter of 57 nm and a thickness of 7.5 µm are shown in Figure 1C. Ag(Ni)/TiO_2-NTs binary catalyst, which is synthesized by the electrochemical method, was synthesized by immersing Ni/TiO_2-NTs in a solution containing Ag, and as can be seen in (Fig. 1D), Ag particles with an average size of 38 nm and a thickness of 3.8 µm were deposited on the Ni/TiO_2-NTs electrode. Figure 2 shows the XRD peaks corresponding to the TiO_2-NTs electrode before and after annealing. It is pretty clear that before annealing, no specific peak is observed, but after annealing, peaks related to electrode crystallization and phase change to the anatase phase are clearly observed.

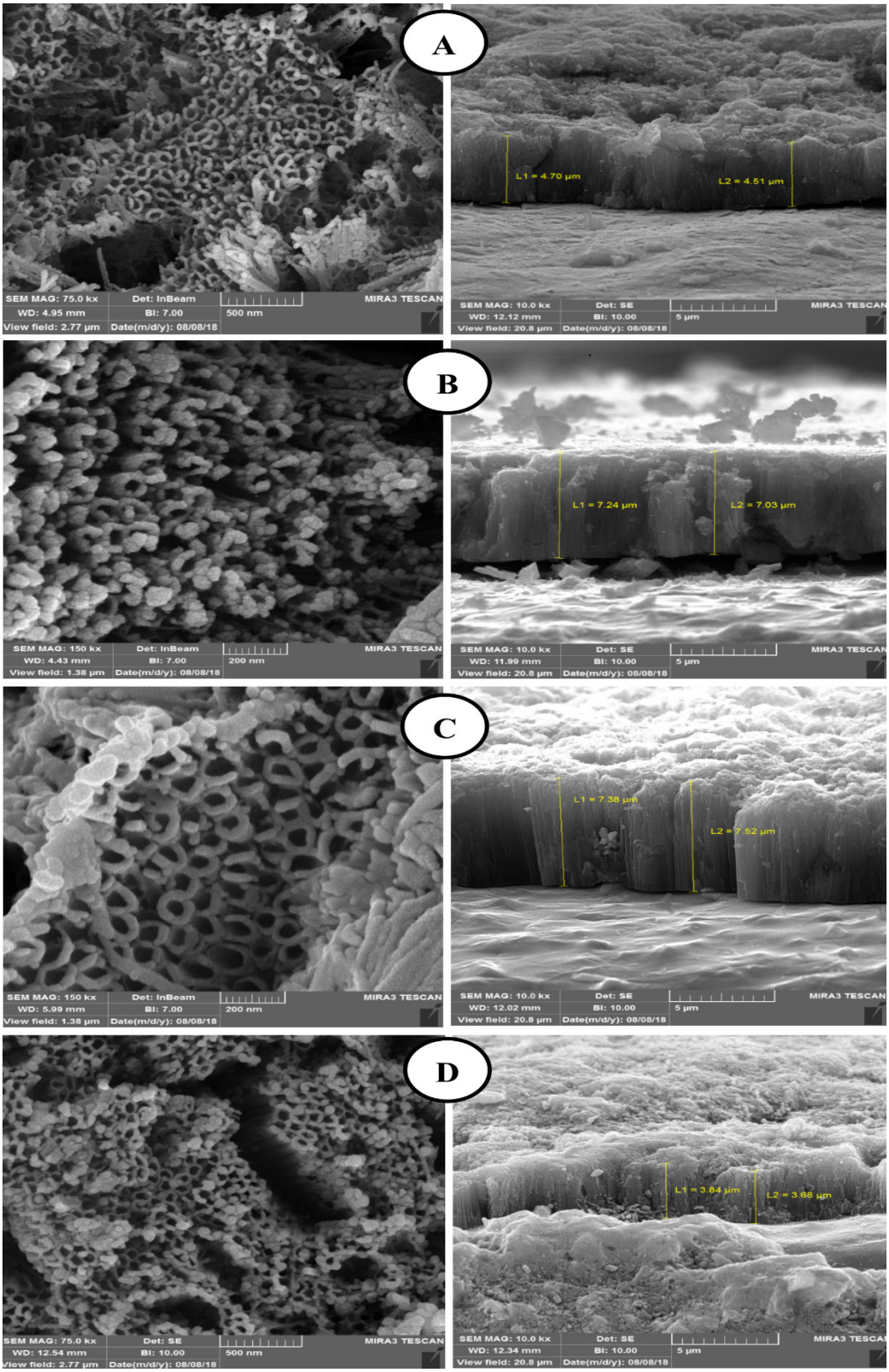

Fig. 1. A) SEM images of TiO_2-NTs electrode with an average diameter of 100 nm and a thickness of 4.7 m, B) SEM images of Ni/TiO_2-NTs electrode with an average diameter of 52 nm and a thickness of 7.3 µm, C) SEM images of Ag/TiO_2-NTs electrode with an average diameter of 57 nm and a thickness of 7.5 µm, D) SEM images of Ag(Ni)/TiO_2-NTs electrode with an average diameter of 38 nm and a thickness of 3.8 µm

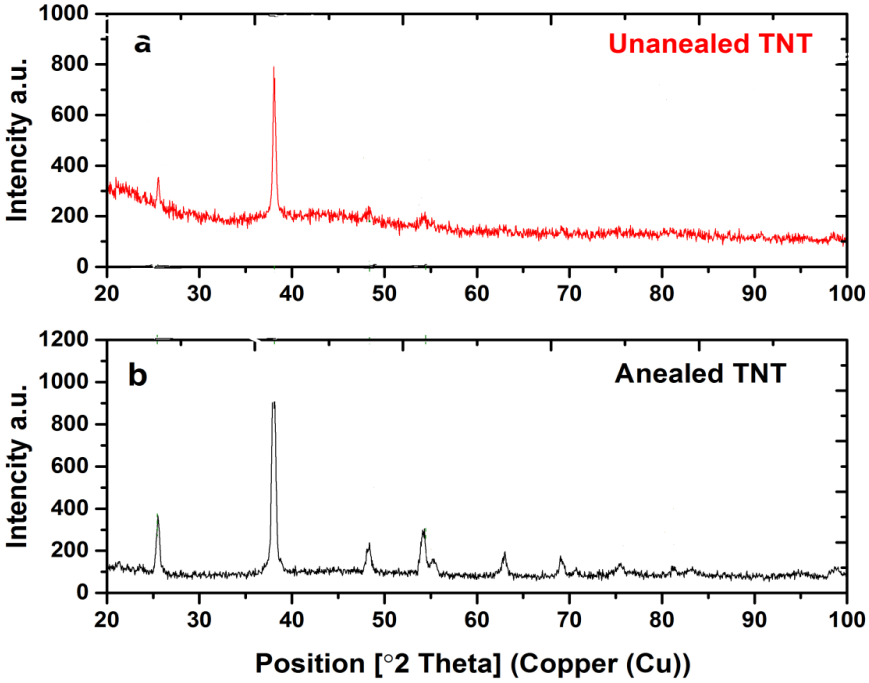

Fig. 2. X-ray diffraction (XRD) pattern of TiO_2-NTs electrode before and after annealing.

3.2. Investigating the electrocatalytic activity

The LSV, CV, CP, and CA analyses of the TiO_2-NTs, Ni/TiO_2-NTs, Ag/TiO_2-NTs, and Ag(Ni)/TiO2-NTs in 1 M KOH solution at different concentrations of NaBH4, at room temperature, and scanning speed 50 mV/S are shown in Figures 3-6. It can be seen that the 0.05 M $NaBH_4$ solution has a higher current and potential than the other three concentrations. Therefore, a final concentration of 0.05 M $NaBH_4$ was chosen for subsequent analyses. The LSV and CV of the synthesized electrodes in 1 M KOH and 0.05 M $NaBH_4$ at room temperature and a scanning speed of 50 mV/S are shown in Figure 7. Also, it can be seen that the Ag(Ni)/TiO_2-NTs catalyst had the highest efficiency and is higher than the other three catalysts.

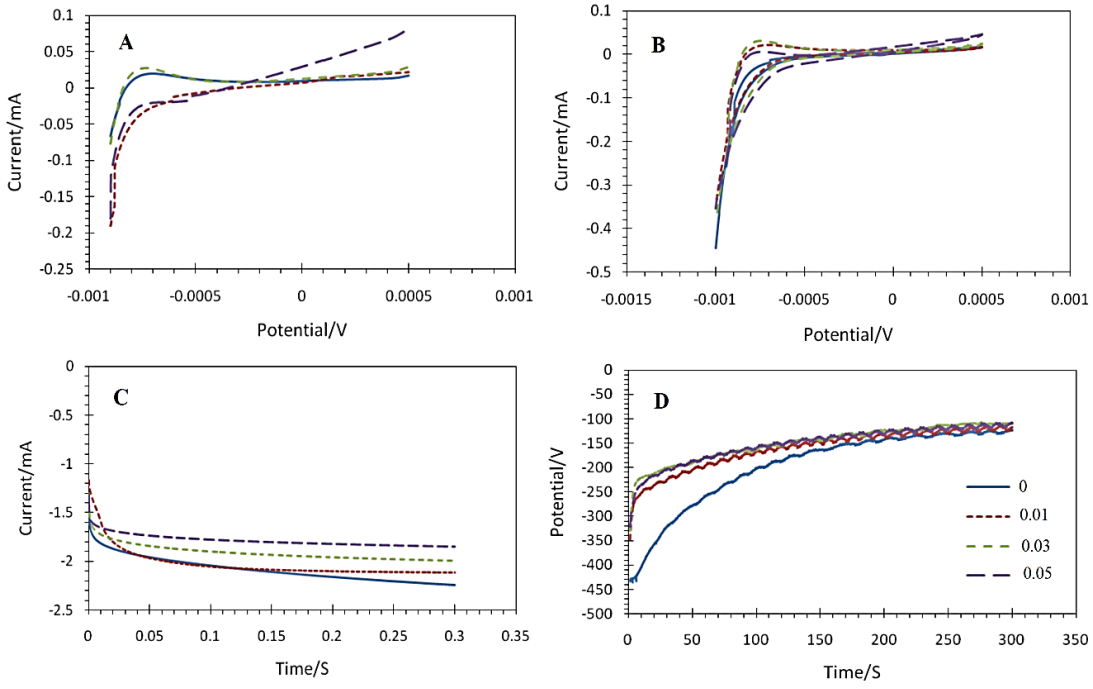

Fig. 3. A) LSV, B) CV, C) CP and D) CA of TiO_2-NTs electrode in 1M KOH solution at different concentrations of $NaBH_4$, 0 50 mV/S and 300 s.

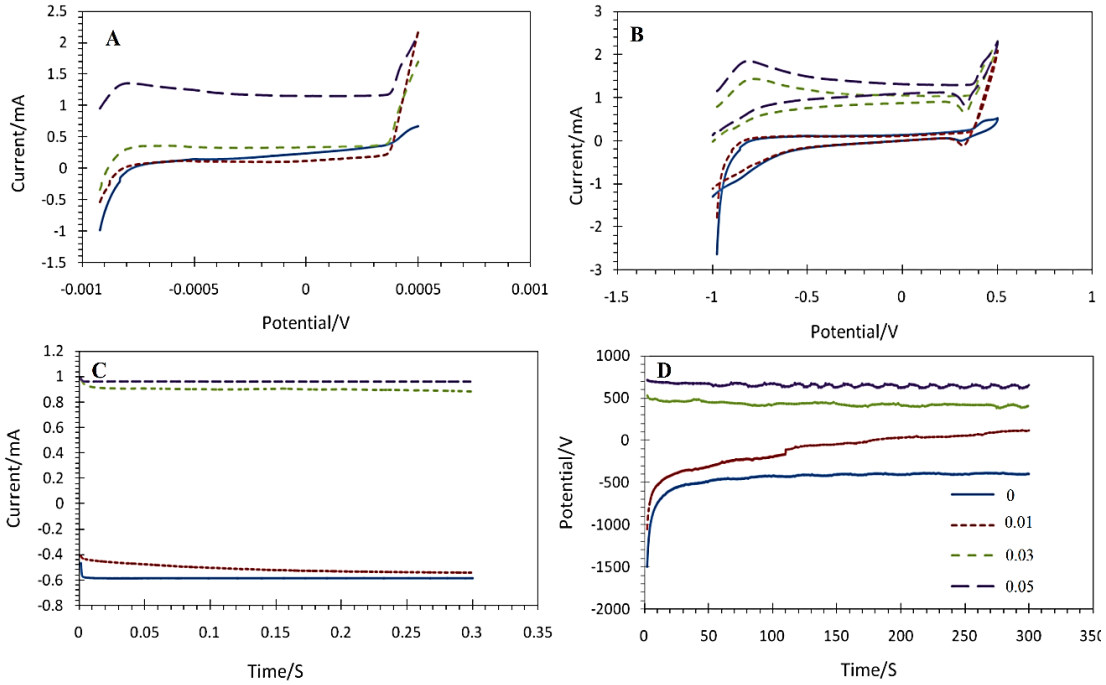

Fig. 4. A) LSV, B) CV, C) CP, D) CA of Ni/TiO_2-NTs electrode in 1M KOH solution at different concentrations of NaBH4, at room temperature, and scanning speed 50 mV/S and 300 s.

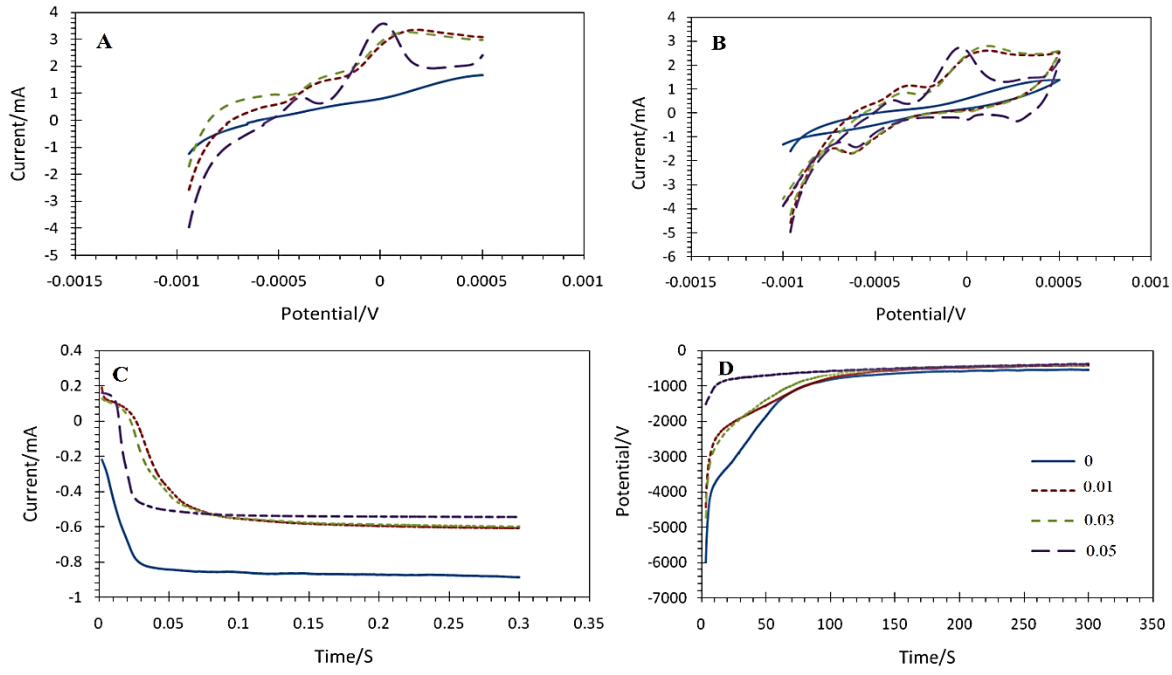

Fig. 5. A) LSV, B) CV, C) CP, D) CA of Ag/TiO_2-NTs electrode in 1 M KOH solution at different concentrations of NaBH4, at room temperature, and scanning speed 50 mV/s and 300 s.

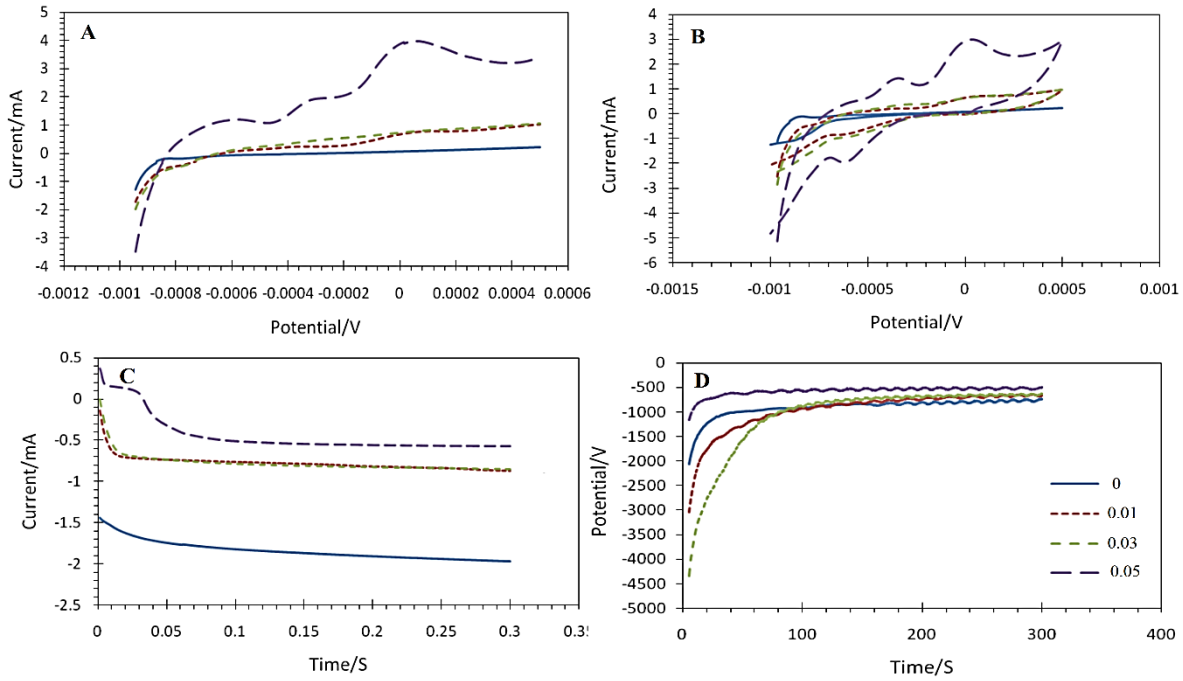

Fig. 6. A) LSV, B) CV, C) CP D) CA of Ag(Ni)/TiO_2-NTs electrode in 1 M KOH solution at different concentrations of $NaBH_4$, at room temperature and scanning speed 50 mV/S and 300 s.

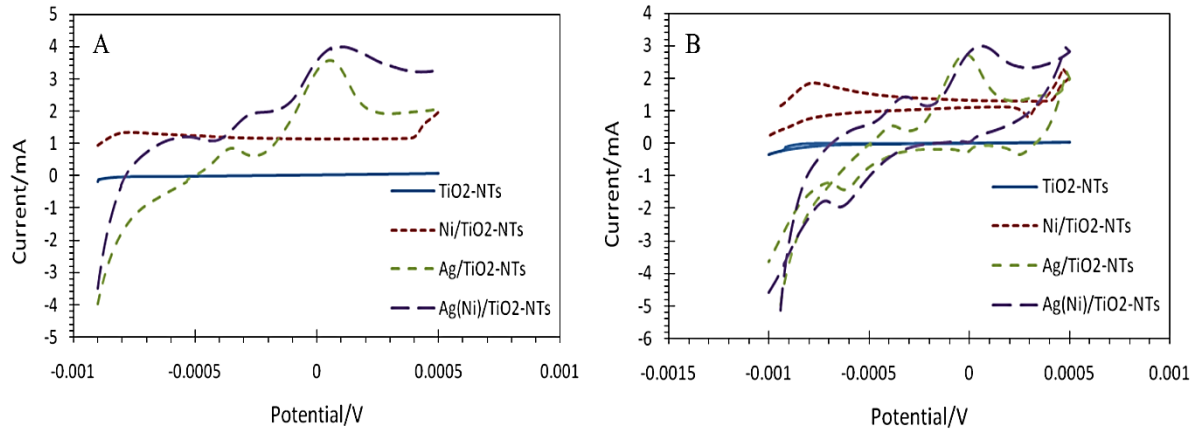

Fig.7. A) LSV and B) of synthesized electrodes in 1 M KOH and 0.05 M $NaBH_4$ at room temperature and scanning speed 50 mV/S and 300 s.

4. Conclusions

In this study, we synthesized nanotubes on the Ti metal surface using a simple and low-cost method (anodizing method). Then, using the electrochemical deposition method, we deposited Ni and Ag layers on the TiO_2-NTs electrode. In the next step, to prepare the Ag(Ni)/TiO_2-NTs electrode, the Ni/TiO_2-NTs electrode was immersed in $AgNO_3$ solution. The structure, morphology, composition, and electrical performance of the fabricated catalysts were investigated using SEM, XRD, LSV, CV, CP, and CA. SEM images and XRD data indicated that the nanotubes were well synthesized, and the Ni, Ag, and Ag(Ni) particles were well dispersed on their surfaces. The results showed that bimetallic electrodes are more efficient in the electrooxidation of borohydrate.

5. Acknowledgments

The authors thank Behbahan Khatam Alanbia University of Technology for its financial support for this work.

6. References

[1] D. M. F. Santos, C. A. C. Sequeira, Sodium borohydride as a fuel for the future, Renew. Sustain. Energy Rev., 15 (2011) 3980-4001. https://doi.org/10.1016/j.rser.2011.07.018

[2] M. M. Momeni, Y. Ghayeb, M. Davarzadeh, Single-step electrochemical anodization for synthesis of hierarchical WO_3–TiO_2 nanotube arrays on titanium foil as a good photoanode for water splitting with visible light, J. Electroanal. Chem., 739 (2015) 149-155. https://doi.org/10.1016/j.jelechem.2014.12.030

[3] M.J.F. Ferreira, F. Coelho, C.M. Rangel, A.M.F.R. Pinto, Batch sodium borohydride hydrolysis systems: Effect of sudden valve opening on hydrogen generation rate, Int. J. Hydrogen Energy, 37 (2012) 1947-1953. https://doi.org/10.1016/j.ijhydene.2011.08.097

[4] R. Ghasemi, B. Kamyab Moghadas, I. Mohammadi, Optimum Ni:Co weight ratio for Pd-Nix-Coy/rGO catalyst nanoparticle for borohydride electro-oxidation in direct borohydride fuel cells, Electrochim. Acta, 512 (2025) 145413. https://doi.org/10.1016/j.electacta.2024.145413

[5] M-K. Nguyen, K. D. Huang, Two-dimensional parametric investigation of zinc-air fuel cell with flowing electrolyte by numerical method, Electrochim. Acta, 513 (2025) 145548. https://doi.org/10.1016/j.electacta.2024.145548

[6] M.C. Sison Escaño, R.L. Arevalo, E. Gyenge, H. Kasai, Electrocatalysis of borohydride oxidation: a review of density functional theory approach combined with experimental validation, J. Phys.: Condens. Matter, 26 (2014) 353001. https://doi.org/10.1088/0953-8984/26/35/353001

[7] Z. Jusys, R.J. Behm, Borohydride oxidation over Pt/C, Au/C and AuPt/C thin-film electrodes studied by rotating disk electrode and differential electrochemical mass spectrometry flow cell measurements, Electrochim. Acta, 513 (2025) 145608. https://doi.org/10.1016/j.electacta.2024.145608

[8] Ş. Karabiberoğlu, Z. Dursun, Au-Pt bimetallic nanoparticles anchored on conducting polymer: An effective electrocatalyst for direct electrooxidation of sodium borohydride in alkaline solution, Mater. Sci. Eng. B, 288 (2023) 116158. https://doi.org/10.1016/j.mseb.2022.116158

[9] L. Yi, W. Wei, C. Zhao, C. Yang, L. Tian, J. Liu, X. Wang, Electrochemical oxidation of sodium borohydride on carbon-supported Pt-Zn nanoparticle bimetallic catalyst and its implications to direct borohydride-hydrogen peroxide fuel cell, Electrochim. Acta, 158 (2015) 209-218. https://doi.org/10.1016/j.electacta.2015.01.111

[10] A. Balčiūnaitė, L. Tamašauskaitė-Tamašiūnaitė, D. M. F. Santos, A. Zabielaitė, A. Jagminienė, I. Stankevičienė, E. Norkus, Au nanoparticles modified Co/Titania nanotubes as electrocatalysts for borohydride oxidation, Fuel Cells, 17 (2017) 690-697. https://doi.org/10.1002/fuce.201600168

[11] D. Cao, Y. Gao, G. Wang, R. Miao, R., Y. Liu, A direct $NaBH_4$–H_2O_2 fuel cell using Ni foam supported Au nanoparticles as electrodes, Int. J. Hydrogen Energy, 35 (2010) 807-813. https://doi.org/10.1016/j.ijhydene.2009.11.026

[12] P. He, X. Wang, Y. Liu, X. Liu, L. Yi, Comparison of electrocatalytic activity of carbon-supported Au–M (M= Fe, Co, Ni, Cu and Zn) bimetallic nanoparticles for direct borohydride fuel cells, Int. J. Hydrogen Energy, 37 (2012) 11984-11993. https://doi.org/10.1016/j.ijhydene.2012.05.054

[13] P. He, X. Wang, P. Fu, H. Wang, L. Yi, The studies of performance of the Au electrode modified by Zn as the anode electrocatalyst of direct borohydride fuel cell, Int. J. Hydrogen Energy, 36 (2011) 8857-8863. http://doi.10.1016/j.ijhydene.2011.04.128

[14] S. Li, L. Wang, J. Chu, J. Zhu, Y. Chen, Y. Liu, Investigation of Au@ Co-B nanoparticles as anode catalyst for direct borohydride fuel cells. Int. J. Hydrogen Energy, 41 (2016) 8583-8588. https://doi.org/10.1016/j.ijhydene.2016.02.128

[15] M.Ghaedi,J.Tashkhourian,M.Montazerozohori, A. Amiri Pebdani, S. Khodadoust, Design of an efficient uranyl ion optical sensor based on 1′-2, 2′-(1, 2-phenylene) bis (ethene-2, 1-diyl) dinaphthalen-2-ol, Mater. Sci. Eng. C, 32 (2012) 1888-1892. https://doi.org/10.1016/j.msec.2012.05.006

[16] S. Khodadoust, M.S. Talebianpoor, Optimization of the extraction of clonazepam and lorazepam using nano-sponge activated carbon and its determination by high-performance liquid chromatography, Microchem. J., 207 (2024) 111937. https://doi.org/10.1016/j.microc.2024.111937

[17] S. Khodadoust, R. Bekhradi Nasab, F. Zeraatpisheh, Ultrasound-assisted dispersive nano sponge-activated carbon for extraction of propoxur and carbaryl: Response surface methodology, J. Water Process Eng., 64 (2024) 105712. https://doi.org/10.1016/j.jwpe.2024.105712

[18] M. Mazloomian, A. A. Ebrahimi, M. Dolatabadi, S. Ahmadzadeh, Removal of p-nitrophenol from industrial wastewater using electrochemical oxidation with Mn-PbO2 electrode: Analysis by high-performance liquid chromatography technique, Anal. Methods Environ. Chem. J., 7 (2024) 5-16. https://doi.org/10.24200/amecj.v7.i04.331

[19] H. Ö. Akduman, E. Özdemir, Zirconia supported bimetallic Co–Mn–B catalyst with superior catalytic activity for hydrolysis of sodium borohydride, Int. J. Hydrogen Energy, 100 (2025) 67-78. https://doi.org/10.1016/j.ijhydene.2024.12.261

[20] K. I. Alabid, H. N. Nasser, Determine methylene blue based on carbon paste electrode modified with nanoparticles of nickel oxide-nitrogen carbon quantum dots and carbon structures by cyclic voltammetry, Anal. Methods Environ. Chem. J., 7 (2024) 17-29. https://doi.org/10.24200/amecj.v7.i01.272

[21] M. Mohammadi Asl, H. Shirkhanloo, N. Mansouri, S.A. Haji Seyed Mirzahosseini, F. Atabi, Functionalized graphene oxide with bismuth and titanium oxide nanoparticles for efficiently removing formaldehyde from the air by photocatalytic degradation–adsorption process, J. Anal. Test., 7 (2023) 444-458. https://doi.org/10.1007/s41664-023-00272-0

[22] A. Faghihi-Zarandi, J. Rakhtshah, B. Bahrami Yarahmadi, H. Shirkhanloo, A rapid removal of xylene vapor from environmental air based on bismuth oxide coupled to heterogeneous graphene/graphene oxide by UV photo-catalytic degradation-adsorption procedure, J. Environ. Chem. Eng., 8 (2020) 104193. https://doi.org/10.1016/j.jece.2020.104193

[23] H. Shirkhanloo, F. Golbabaei, A. Vahid, A. Faghihi Zarandi, A novel nano-palladium embedded on the mesoporous silica nanoparticles for mercury vapor removal from air by the gas field separation consolidation process, Appl. Nanosci., 12 (2022) 1667-1682. https://doi.org/10.1007/s13204-022-02366-0

[24] M. Khaleghi Abbasabadi, Speciation of cadmium in human blood samples based on Fe_3O_4-supported naphthalene-1-thiol- functionalized graphene oxide nanocomposite by ultrasound-assisted dispersive magnetic micro solid phase extraction, J. Pharm. Biomed. Anal., 189 (2020)113455. https://doi.org/10.1016/j.jpba.2020.113455